HENRY

Hydraulic Engineering Repository

Ein Service der Bundesanstalt für Wasserbau

Article, Published Version

Kersten, Thomas P.; Lindstaedt, Maren; Mechelke, Klaus
Coastal cliff monitoring using UAS photogrammetry and TLS

Hydrographische Nachrichten

Coastal cliff monitoring using UAS photogrammetry and TLS

A peer-reviewed paper by THOMAS P. KERSTEN, MAREN LINDSTAEDT and KLAUS MECHELKE

Climate change and the imminent sea-level rise mean that coastal protection is becoming increasingly important, and measures must be taken to ensure that life and important infrastructure in coastal areas are protected. An essential prerequisite for the implementation of appropriate coastal protection measures is the monitoring of endangered areas through appropriate sensor technology for the documentation and quantification of damages caused. In this contribution, a practical application is introduced using low-cost UAS (unmanned aerial system) to perform aerial flights for the monitoring of a coastal cliff at the Baltic Sea in Germany, since cliffs are exposed to and unprotected from autumn and winter storms. In comparison to UAS-based photogrammetric monitoring with terrestrial laser scanning (TLS), the photogrammetric method showed the same accuracy, but better coverage of the investigated area and a more efficient workflow.

3D | comparison | erosion | dense image matching | DSM | landslide
3D | Vergleich | Erosion | Dense-Image-Matching | DSM | Erdrutsch

Wegen des Klimawandels und des bevorstehenden Meeresspiegelanstiegs wird der Küstenschutz immer wichtiger. Mit zahlreichen Maßnahmen werden Leben und wichtige Infrastrukturen in den Küstengebieten geschützt. Eine wesentliche Voraussetzung für die Umsetzung entsprechender Küstenschutzmaßnahmen ist die Überwachung der gefährdeten Gebiete durch geeignete Sensorik zur Dokumentation und Quantifizierung der verursachten Schäden. In diesem Beitrag wird eine praktische Anwendung vorgestellt, bei der ein Küstenkliff an der Ostsee, das ungeschützt und exponiert gegenüber Herbst- und Winterstürmen ist, mit Hilfe von kostengünstigen UAS (unbemannten Flugsystemen) überwacht wurde. Ein Vergleich des luftgestützten photogrammetrischen Monitorings mit terrestrischem Laserscanning (TLS) zeigte, dass die photogrammetrische Methode die gleiche Genauigkeit aufweist, aber eine bessere Abdeckung des Untersuchungsgebiets und einen effizienteren Arbeitsablauf ermöglicht.

Authors

Prof. Dr. Thomas P. Kersten teaches photogrammetry and laser scanning at HafenCity University (HCU) in Hamburg. Maren Lindstaedt and Klaus Mechelke are research associates at HCU.

thomas.kersten@hcu-hamburg.de

1 Introduction

Due to climate change and the consequent rise of sea level, coastal areas are increasingly at risk from extreme weather events such as storm-induced flooding, which can lead to increased coastal erosion. According to Alexander (1993), the natural potential for coastal erosion is influenced by the following five factors: (1) the lack of protection of rocks and sediments against waves and currents, (2) the topography of the coast, (3) the tidal range and the intensity of currents, (4) the coastal climate and (5) the (lack of) sediment supply. In addition, coastal erosion may be enhanced by anthropogenic modifications such as the removal of vegetation and other materials (e.g. sand).

In order to document, analyse and evaluate the damage to coastal objects and structures, geodetic surveying techniques such as terrestrial and airborne laser scanning or aerial photography and UAS (unmanned aerial system) photogrammetry are increasingly used today, depending on the size of the area. However, the idea is not new. In earlier works, for example, Mills et al. (2005) pre-

sent a solution, based on two component technologies – the Global Positioning System (GPS) in kinematic mode and digital small format aerial photogrammetry for change detection between temporal data epochs for a rapidly eroding coastline (Filey Bay, North Yorkshire, England). Many years later terrestrial laser scanning (TLS) became a popular technology for these tasks. For example, the use of TLS for monitoring coastal rocks on the island of Rügen, Germany, and the analysis of mass movements is presented in Kuhn and Prüfer (2014). Tschirschwitz et al. (2016) present a TLS-based monitoring system for the deformation analysis of groynes (also known as wing dykes used as hard coastal protection structures) at the River Elbe. Lim et al. (2005) use terrestrial photogrammetry in combination with TLS for cliff monitoring. Michoud et al. (2015) present a study for testing boat-based mobile LiDAR capabilities by scanning 3D point clouds of unstable coastal cliffs along Dieppe coastal cliffs in High Normandy, France. In one research project, Tiepolt (2016) investigated mobile laser scanning and the use

of UAS for recording coastal areas and protective structures on the North and Baltic Seas.

Today, UAS are increasingly being used for the acquisition of coastal data and objects due to their cost efficiency and high flexibility. Traut (2017) describes their investigations with the high-end fixed-wing UAS Q-200 with post-processing kinematic (PPK) from the company QuestUAV. In the aforementioned study, UAS photogrammetry is successfully used without control points to measure long-term erosion along the Northumberland coast in northeastern England. Another example of the use of UAS photogrammetry with a DJI S1000 octocopter is described by Barlow et al. (2017). They generate point clouds and spectral data for the kinematic analysis of the chalk cliffs in Telscombe – a rock face of about 750 m length and 20 to 49 m height east of Brighton in England. Dewez et al. (2016) also use UAS imagery to generate very high-resolution point clouds in order to document small-scale changes in a chalk cliff at the English Channel coast. Further research on the use of UAS for the monitoring of coastal landslides and environments can be found in Esposito et al. (2017) and Irvine et al. (2018). Since 2016, the Lower Saxon State Office for Water Management, Coastal and Nature Conservation (Niedersächsischer Landesbetrieb für Wasserwirtschaft, Küsten- und Naturschutz, NLWKN) has been using a fixed-wing UAS for surveying and documenting the coastlines of the German North Sea coast (Dirks 2018).

This paper describes the use of two low-cost UAS systems from DJI for aerial flights over a natural coastal object, the Brodten cliff at the Baltic Sea, by the Laboratory for Photogrammetry & Laser Scanning of the HafenCity University Hamburg. The monitoring of the Brodten cliff started in 2004 with terrestrial laser scanning as a study project for students and continued until 2016 using a variety of different laser scanning systems. Since 2016 UAS-based aerial image data have been used three times for photogrammetric monitoring of the Brodten cliff. The temporal changes of the cliff have been documented and quantified from 2004 until 2020 through comparisons of the 3D surface models from different periods. Results of the UAS-based monitoring were visualised and the 2016 data set was compared to corresponding TLS data with respect to the criteria coverage, accuracy and efficiency.

2 The Brodten cliff

The Brodten cliff is a steep coast, upwards of 4 km long, located on the Bay of Lübeck (Baltic Sea) between Travemünde and Niendorf in Schleswig-Holstein. Due to the onset of glacial melting during the last ice age, a huge glacier tongue formed the present-day bay, where sandy sediments, marl and human-sized erratic blocks transported by the glacier were deposited in a moraine, forming the

Fig. 1: The coastal cliff at Brodten with the Hermannshöhe restaurant in the background, photographed from the DJI UAS on 20 January 2020

outline of the current Baltic Sea coast (Schmidtke 1992). The coastline, in places up to 20 m high, is in large sections still an active cliff. It recedes on average up to one metre per year due to the erosive action of waves generated by east-northeast winter storms, heavy rainfall with the accompanying softening and washing out of sediment layers, as well as freezing seepage water spreading in volume. In the immediate vicinity of the steep bank is the restaurant Hermannshöhe, built before the First World War and replaced by a new building in May 2012, which is a popular destination for tourists. The HCU Hamburg carried out coastal cliff monitoring with terrestrial laser scanners in Hermannshöhe section (Fig. 1) between 2004 and 2016 in order to document the changes and landslides. In 2016 the steep coast was surveyed with a UAS for the first time (Kersten and Lindstaedt 2017) followed by a second survey with the same UAS in 2018 (Kersten et al. 2019). Fig. 1 shows the investigation area at the Brodten cliff with the restaurant building in the background, located some 52 m from the edge of the cliff (status January 2020).

3 Systems used

Different terrestrial laser scanning systems were used for the documentation and monitoring of the Brodten cliff section over twelve years (Fig. 2 and Table 1).

Following comparison of terrestrial laser scanning and UAS photogrammetry for the monitoring of the cliffs, it was decided to continue the

Fig. 2: Terrestrial laser scanning at the coastal cliff of Brodten – Z+F IMAGER 5003 (2004), Mensi GS100 (2005), Riegl VZ-400 (2010) and Faro Focus3D X330 and Z+F IMAGER 5010 (2016)

Period	Date	Scanner	Scan station
0	15.03.2004	Mensi GS100 and Z+F IMAGER 5003	3 and 11
1	03.06.2005	Mensi GS100	6
2	22.06.2006	Mensi GS100	7
3	13.11.2007	Mensi GS100	3 (21 scans)
4	17.08.2009	Mensi GS100 and Z+F IMAGER 5006i	2 and 6
5	02.06.2010	Riegl VZ-400	8
6	21.06.2016	Z+F IMAGER 5010 (top) and Faro Focus3D X330 (bottom)	5 and 8

Table 1: Terrestrial laser scanning at the Brodten cliff – periods, dates and scanner

	DJI Phantom 3 Advanced	DJI Phantom 4 Pro KlauPPK
Camera	Sony Exmor	Zenmuse X4S
Lens	Integrated 4.0/2.8	Integrated 8.8/2.8
Sensor	CMOS	CMOS
Shutter	Rolling	Global
Resolution [MP]	12.4	20
Sensor size [mm]	6.16 × 4.62	13.2 × 8.8
Image resolution	4000 × 3000	5472 × 3648
Pixel size [μm]	1.54	2.4
Focal length [mm]	4.0	8.8

Table 2: Technical specification of both cameras: DJI Phantom 3 Advanced and DJI Phantom 4 Pro

documentation of the cliff only by UAS systems due to higher efficiency. For this task low-cost UAS systems from DJI were used: Phantom 3 Advanced with a fixed 12 MP camera (www.dji.com/de/phantom-3-adv) and the Phantom 4 Pro KlauPPK with the 20 MP camera X4S (klauppk.com/hardware/) allowing the precise determination of each image position from GNSS in a post-processed kinematic (PPK) mode using the KlauPPK software from Klau Geomatics (Australia). The key technical data of the DJI Phantom 3 Advanced and the associated camera are summarised in Kersten et al. (2019), but the technical specifications of the cameras of both DJI Phantom are listed in Table 2. The Phantom 4 Pro,

Fig. 3: DJI Phantom 4 Pro KlauPPK (left), remote control with Apple iPad (centre) and signalised ground control point (right)

including remote control and signalised ground control points, is illustrated in Fig. 3. The central component of the KlauPPK hardware is the multi-channel multi-frequency GNSS receiver of NovAtel. The KlauPPK software provides sophisticated PPK data processing to determine the precise coordinates of the projection centre of each image taken in the requested coordinate system.

4 Data acquisition and aerial triangulation

While the Brodten cliff has been surveyed seven times by different terrestrial laser scanning systems on various scan stations between 2004 and 2016, the UAS system DJI Phantom flew over the cliff three times: on 21 June 2016, 10 December 2018 (both DJI Phantom 3 Advanced) and 20 January 2020 (DJI Phantom 4 Pro). The DJI Phantom 3 was manually controlled during the aerial flights over the section of the steep bank, whereby vertical and oblique images were taken. For the DJI Phantom 4 two automatic nadir aerial flights were conducted, in addition to a manual controlled flight for oblique images. The technical data of the three aerial flights including the flight date, flight duration, number of photos, average flight altitude and flight speed, pixel size on the ground and number of control points are summarised in Table 3. The average flight speed was estimated from the distance flown, which was calculated from the spatial positions of each photo, and the flight duration.

Signalised ground control points (GCP) with a target diameter of 10 cm were well distributed in object space and then determined with geodetic surveying methods using three fixed reference points close to the restaurant. While all control points in each period from 2004 until 2016 were determined by a Leica total station in a geodetic network with a standard deviation of 1 to 2 cm, the coordinates of the control points at the top and bottom of the cliff were determined in the UTM coordinate system by RTK-GNSS Trimble R8s and the correction data service Trimble VRS Now with a standard deviation of 1 to 2 cm. However, Trimble specifies the accuracy of single points with 1 to 2 cm in XY and 2 to 4 cm in Z for VRS Now (SITECH 2020).

The determination of the adjusted image orientation and camera calibration were carried out in a bundle block adjustment using the software Agisoft PhotoScan (version 1.4.4) and Metashape (version 1.5.5). Therefore, the coordinates of image orientation, only for the aerial flight in 2020, which were computed from the PPK observations, were introduced into the bundle block adjustment as weighted observations with an accuracy of ±3 cm. All pixel coordinates of correlating image points were automatically measured in all photos used. The reference to the geodetic coordinate system was established by manual measurements of the

System	Flight date	Flying time [min]	Number of photos	Average flying height [m]	Average flight speed [m/s]	Ground sampling distance [mm]	Number of ground control points
DJI Phantom 3 Advanced	21.06.2016	15	170	20.1	0.8	10.7	15
DJI Phantom 3 Advanced	10.12.2018	26	186	29.1	1.3	6.8	12
DJI Phantom 4 Pro KlauPPK	10.02.2020	27	174	20.3	1.3	7.9	9

Table 3: Technical specification of the UAS-based flight data

signalised control points in the respective images of each aerial flight. The configuration of nine GCP for the aerial flight in 2020 is illustrated in Fig. 4 (bottom). During each aerial UAS flight, a very high overlap of more than nine images per area could be achieved for all photogrammetric blocks.

Table 4 shows the results of aerial triangulation, giving average deviations at the ground control points of less than 1 cm for all UAS flights, a sufficient result for this particular monitoring task. The slightly higher deviations for the image block recorded in January 2020 are probably due to a bad signalling of the control points and their geodetic measurements. The projection error (last two columns of Table 4) is a criterion for the quality of the automatic pixel measurements. For these aerial triangulations the projection error is 1/4 to 1/6 pixel with maximum values below one pixel, indicating a good result. In an adjustment without control points, the following deviations are achieved at the nine check points for the UAS aerial flight 2020: X = 2.8 cm, Y = 1.8 cm and Z = 5.5 cm. However, if only one control point is used to support the height in the adjustment, the result at the eight check points is slightly better: X = 2.0 cm, Y = 1.4 cm and Z = 3.8 cm. These two results demonstrate that it would be possible to carry out the project without control points when performing an UAS-based aerial flight with RTK or PPK. However, it is recommended to always use at least one control point for the adjustment of image observations of RTK/PPK aerial flights.

5 Generation of digital surface models

After the determination of image orientation and camera calibration, a dense point cloud was generated with PhotoScan (2016 and 2018) and Metashape (2020) with the following parameters: quality medium (corresponds to an image reduction by factor 4) and filtering aggressive to eliminate gross errors. The generated point clouds were then manually cleaned and the area of interest

Fig. 4: 3D meshed models of the Brodten Cliff derived from UAS-based aerial imagery – June 2016 (top), December 2018 (centre) and January 2020 (bottom) including the configuration of nine ground control points (yellow dots with blue flags)

System	Flight date	Number of photos	Number of ground control points	$|s_x|$ [mm]	$|s_y|$ [mm]	$|s_z|$ [mm]	$s_{x'y'}$ [pixels]	RMS PE [pixels]	Max PE [pixels]
DJI Phantom 3 Advanced	21.06.2016	170	15	6.4	6.9	7.8	1.06	0.25	0.85
DJI Phantom 3 Advanced	10.12.2018	186	12	5.4	8.4	7.4	1.12	0.20	0.71
DJI Phantom 4 Pro KlauPPK	10.02.2020	174	9	8.0	6.7	18.1	0.54	0.15	0.47

Table 4: Results of aerial triangulation for three UAS-based photogrammetric image blocks
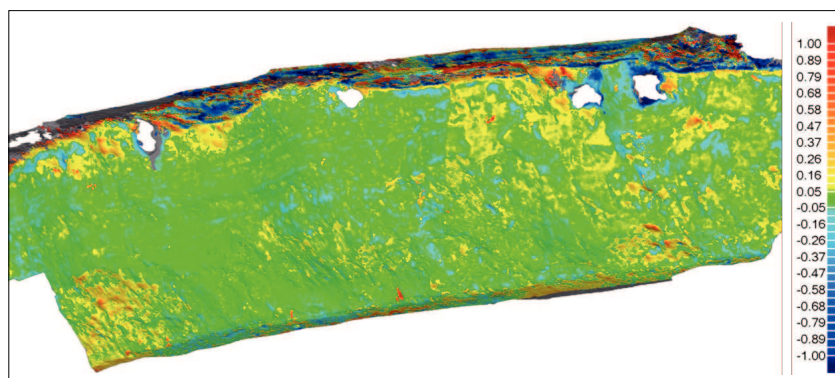
Fig. 5: 3D comparison of 3D meshed models derived from TLS and UAS-based aerial imagery in the year 2016 – differences higher than ±5 cm (green) are indicated in different colour (reddish or bluish)

segmented. For the reduced point cloud, Photo-Scan/Metashape calculated a triangular mesh in high resolution, which represents a digital surface model (DSM). Fig. 4 shows the three generated 3D surface models of the cliff after texture mapping using the colour images.

6 Cliff monitoring

The 3D point clouds from different periods generated from TLS and UAS photogrammetry data were then used to document the changes in Geomagic Control. To evaluate the quality of the UAS data, a 3D comparison between the 3D models from terrestrial laser scanning and from the UAS image flight, both from the same day in 2016, was also calculated. The deviations between the two 3D models are visualised as colour-coded in Fig. 5. Most of the deviations between TLS and UAS are in the range of ±5 cm (green), so that the results from UAS image data are comparable with the TLS data. The achieved accuracy for the digital surface model of a few centimetres is therefore more than sufficient for the evaluation of the cliff monitoring, i.e. both methods meet the requirements for cliff monitoring, since the deviations are on average up to one metre per year. Especially in the areas of vegetation, higher deviations are visible between both data sets, since TLS is mostly able to penetrate the vegetation, while all automatic image

point measurements in the photos are on top of the vegetation.

The time required to survey the coastal section in 2016 using terrestrial laser scanning (including ground control point signalisation and surveying by tachymetry) by up to ten students and two scanners was approximately five hours, while the UAS image flights took only up to 25 minutes. Together with the control point measurement by the RTK-GNSS Trimble R8s, a two-man team needed only 2.5 hours on site (2018 and 2020). If the evaluation of the laser scan data (registration and georeferencing of the scans, filtering, meshing and 3D comparison) takes one working day (estimated), the results of the UAS image flight are available after only half a working day if a powerful computer is available. This is a reduction of the workload by a factor of 2.

As monitoring for the cliff in Brodten by terrestrial laser scanning (TLS) and recently by UAS photogrammetry has been carried out since 2004, results from previous investigations are already available (Qualmann 2010; Kersten and Lindstaedt 2017; Kersten et al. 2019). The visualisation of the two 3D comparisons in Fig. 6 shows massive erosion (blue colour) for the cliff section in the period between 2016 and 2020 (left), while erosion between 2018 and 2020 is significantly less (right), as expected due to the shorter period of 13 months.

In Fig. 7 the changes at the cliff are visualised by coloured virtual edge profiles at 18 m and 1.5 m height from 2004 to 2020. The rearrangement of the footpath due to variation in the position of the cliff edge can also be seen quite well in this figure. According to Fig. 7, the retreat of the cliff edge from 2004 until 2020 (190 months or 15.8 years) ranges between 90 cm and 50 cm per year (at the 18-m profile close to the edge of the cliff).

7 Conclusions and outlook

In this article it was demonstrated that aerial flights with low-cost UAS systems are very suitable for the monitoring of coastal areas and objects, since they guarantee a high resolution of the data including
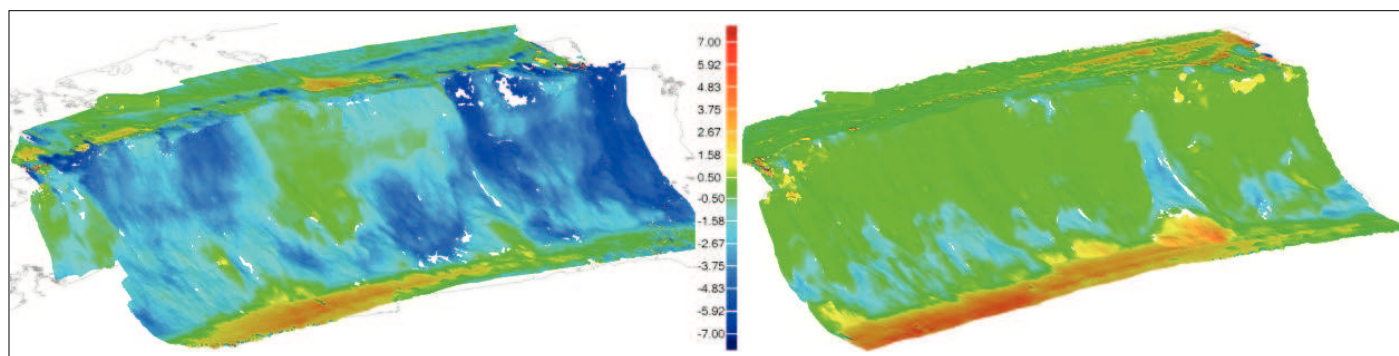

Fig. 6: 3D comparison of 3D meshed models derived from UAS-based aerial imagery: 2016-2020 (left) and 2018-2020 (right)
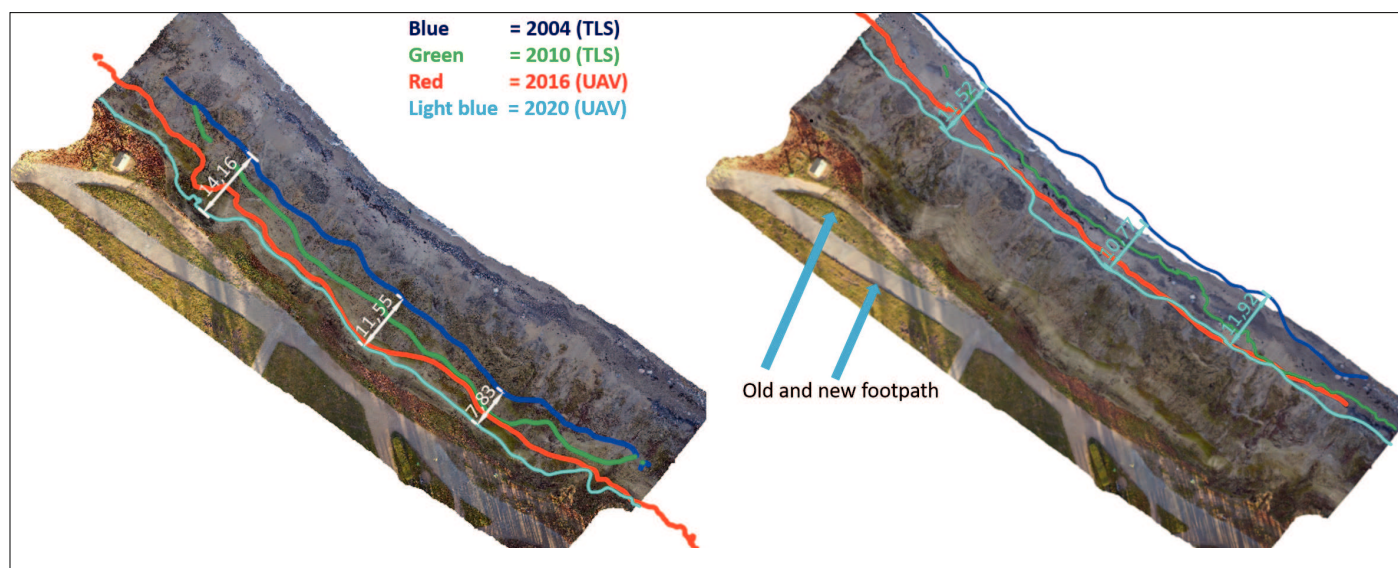
Fig. 7: Temporal changes at the Brodten cliff from 2004 until 2020 documented by coloured profiles at the height 18 m (left) and at the height 1.5 m (right) including distances of the profiles between 2004 and 2020 at selected positions for the documentation of the damages

sufficient accuracy. The comparison of the data acquisition and processing using TLS and UAS photogrammetry showed an estimated doubling in speed of project processing due to the short aerial flights and the automated image-based generation of point clouds and surface models. The achievable accuracies for the products (surface models) from the UAS image flights correspond to those of terrestrial laser scanning. However, the optimal recording geometry of images with the UAS flights provides better coverage of the area under investigation.

A comparison of the system costs turns out in favour of the low-cost UAS system, as the computer, software and UAS (here the new DJI Phantom 4 RTK) are significantly cheaper, at approximately EUR 12 000, when compared to a terrestrial laser scanning system at approximately EUR 50 000. Thus, UAS systems are more flexible, faster and cheaper than terrestrial laser scanners for applica-
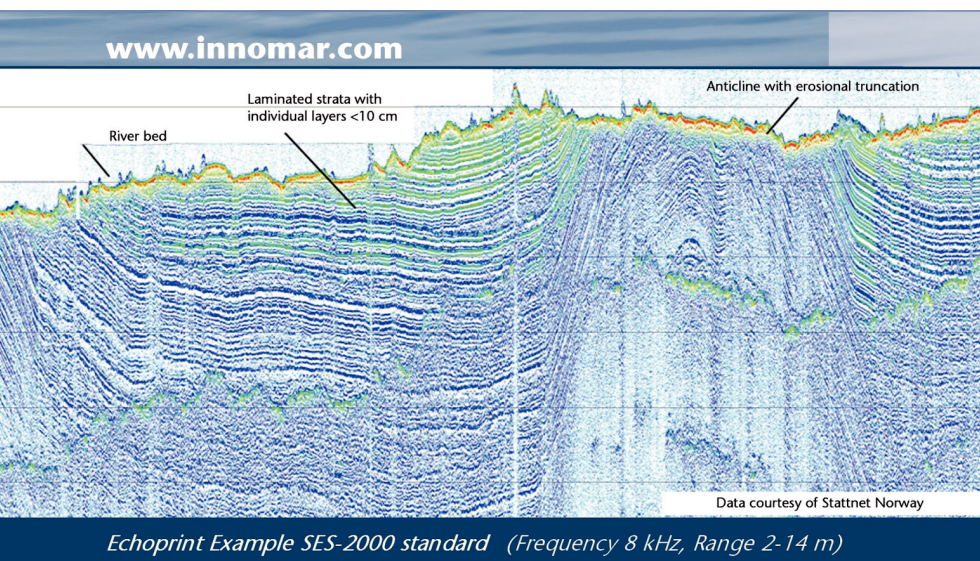
tions in small-scale coastal monitoring. Today, a significant reduction of control points is possible using UAS systems with RTK-GNSS on-board or using the RTK data in a post-processed kinematic mode (PPK), which reduces the time for data acquisition in the field due to reduced ground control signalisation and measurements. The UAS flights should be performed in the winter period to determine a better surface model due to the non-existent green vegetation.

The monitoring of the investigated Brodten cliff has shown that the steep coast is severely damaged by erosion of autumn and winter storms and loses significant mass every year. Further UAS-based aerial flights will be carried out in the future to continue documenting the damages as part of the study project of HCU Hamburg. However, the continuous erosion of the cliff will have drastic consequences for the restaurant only in about estimated 50 years. //

References

Alexander, David (1993): Natural Disasters. UCL Press, London

Barlow, John; Jamie Gilham; Ignacio Ibarra Cofrā (2017): Kinematic analysis of sea cliff stability using UAV photogrammetry. International Journal of Remote Sensing, DOI: 10.1080/01431161.2016.1275061

Dewez, Thomas. J. B.; Jérôme Leroux; Stéphane Morelli (2016): Cliff collapse hazard from repeated multicopter UAV acquisitions: Return on experience. International Archives of the Photogrammetry, Remote Sensing & Spatial Information Sciences, DOI: 10.5194/isprsarchives-XLI-B5-805-2016

Dirks, Holger (2018): UAV für eine effiziente Vermessung im Insel- und Küstenschutz. In: UAV 2018 – Vermessung mit unbemannten Flugsystemen, Schriftenreihe des DVW, Band 89, Wißner-Verlag, Augsburg, pp. 117–122

Esposito, Guiseppe; Riccardo Salvini et al. (2017): Multitemporal monitoring of a coastal landslide through SfM-derived point cloud comparison. The Photogrammetric Record, DOI: 10.1111/phor.12218

Irvine, Mike; Gregg Roberts; L. P. Oldham (2018): Assessing the applicability of unmanned aerial vehicle (UAV) data in environmental monitoring of coastal environments: St. David's, Newfoundland. Current Research (2018) Newfoundland and Labrador Department of Natural Resources Geological Survey, Report 18-1, pp. 15–30

Kersten, Thomas; Maren Lindstaedt (2017): Photogrammetrie auf Knopfdruck – Auswertung und Resultate UAV-gestützter Bildflugdaten. ZfV – Zeitschrift für Geodäsie, Geoinformation und Landmanagement, DOI: 10.12902/zfv-0145-2016

Kersten, Thomas; Maren Lindstaedt et al. (2019): UAV-gestütz-te Bildflüge für das photogrammetrische Monitoring einer Buhne und einer Steilküste. In: Thomas Luhmann; Christina Schumacher (Hrsg.): Photogrammetrie, Laserscanning, Optische 3D-Messtechnik – Beiträge der Oldenburger 3D-Tage 2019, Wichmann, VDE Verlag, Berlin und Offenbach, pp. 222–235

Kuhn, Dirk; Steffen Prüfer (2014): Coastal cliff monitoring and analysis of mass wasting processes with the application of terrestrial laser scanning: A case study of Rügen, Germany. Geomorphology, DOI: 10.1016/j.geomorph.2014.01.005

Lim, Michael; David N. Petley et al. (2005): Combined digital photogrammetry and time-of-flight laser scanning for monitoring cliff evolution. The Photogrammetric Record, DOI: 10.1111/j.1477-9730.2005.00315.x

Michoud, Clément; Dario Carrea et al. (2015): Landslide detection and monitoring capability of boat-based mobile laser scanning along Dieppe coastal cliffs, Normandy. Landslides, DOI: 10.1007/s10346-014-0542-5

Mills, Jon P.; Simon John Buckley et al. (2005): A geomatics data integration technique for coastal change monitoring. Earth Surface Processes and Landforms, DOI: 10.1002/esp.1165

Qualmann, Dorina (2010): Untersuchungen der Hangrut-schungen am Brodtener Steilufer mittels verschiedener Laserscanverfahren. Unveröffentlichte Masterarbeit im Studiengang Geomatik an der HafenCity Universität Hamburg

Schmidtke, Kurt-Dietmar (1992): Entstehung der Küstenmor-phologie der Lübecker Bucht. In: Manfred Diehl (Hrsg.): Lübecker Bucht und Untertrave, Berichte des Vereins Natur und Heimat und des Naturhistorischen Museums zu Lübeck, Heft 23/24

SITECH (2020): Trimble VRS Now. www.sitech.de/fileadmin//user_upload/SITECH_Trimble_VRS_Now_web.pdf, last access 24 April 2020

Tiepolt, Lars (2016): Mobiles Laserscanning und Einsatz von Drohnen zur Aufnahme von Küstengebieten und Küsten-schutzbauwerken. Die Küste, 84, pp. 147–192

Traut, Kerstin (2017): UAV monitoring of coastal erosion. Geomatics World, 25, pp. 19–20

Tschirschwitz, Felix; Klaus Mechelke et al. (2016): Monitoring and deformation analysis of groynes using TLS at the river Elbe. The International Archives of the Photogrammetry, Remote Sensing and Spatial Information Sciences, DOI: 10.5194/isprsarchives-XLI-B5-917-2016